The Journal of Experimental Biology 213, 318-330
Published by The Company of Biologists 2010
doi:10.1242/jeb.031872

The influence of strain and activation on the locomotor function of rat ankle extensor muscles

E. F. Hodson-Tole[1,*] and J. M. Wakeling[2]

[1]The Structure and Motion Laboratory, The Royal Veterinary College, Hawkshead Lane, North Mymms, Hatfield, Hertfordshire, AL9 7TA, UK and [2]Department of Biomedical Physiology and Kinesiology, Simon Fraser University, Burnaby, British Columbia, Canada, V5A 1S6

*Author for correspondence at present address: Institute for Biomedical Research into Human Movement and Health, Manchester Metropolitan University, Manchester, UK (e.tole@mmu.ac.uk)

Accepted 30 September 2009

SUMMARY

The ankle extensor muscles of the rat have different mechanical and physiological properties, providing a means of studying how changes in locomotor demands influence muscle fascicle behaviour, force and mechanical power output in different populations of muscle fibre types. Muscle fascicle strain, strain rate and activation patterns in the soleus, plantaris and medial gastrocnemius muscles of the rat were quantified from sonomicrometric and myoelectric data, collected during treadmill locomotion under nine velocity/incline conditions. Significant differences in peak-to-peak muscle fascicle strains and strain rates were identified between the three muscles ($P<0.001$, all cases), with much smaller strains (<0.1) and strain rates (<0.5 s^{-1}) occurring in soleus and plantaris compared with medial gastrocnemius (>0.2 and >1.0 s^{-1}, respectively). The proportion of stride duration that each muscle was active (duty cycle) differed between locomotor conditions as did the timing of the activation and deactivation phases. A simple Hill-based muscle model was used to determine the influence of muscle activation relative to maximum fascicle strain and duty cycle on total force production and mechanical power output, from a slow and a fast muscle fibre, simulated through two peak-to-peak strain cycles (0.1 and 0.3). The predictions of the model did not complement conclusions that may be drawn from the observation of myoelectric timing and fascicle strain trajectories in each of the muscles. The model predicted that changes in mechanical power output were more sensitive to changes in activation parameters than to changes in strain trajectories, with subtle changes in activation phase and duty cycle significantly affecting predicted mechanical power output.

Key words: skeletal muscle, sonomicrometry, mechanical power, locomotion.

INTRODUCTION

The intrinsic properties of a muscle can be split into three main categories: (1) the stress–strain relationship; (2) the stress–strain rate relationship; and (3) activation–deactivation kinetics. Measurement of these properties typically occurs *in vitro* during isotonic loading of fully activated isolated muscle, small fibre bundles or single fibres. Such information has revealed much about muscle function, and has provided an initial insight into the diversity and similarity that exists between muscles proposed to fulfil specific roles during a range of motor tasks. The loading conditions under which these properties are defined are, however, very simple and do not generally represent patterns of loading, activation and length changes that occur *in vivo*. Improving understanding of the mechanical behaviour of muscles *in vivo*, therefore, depends on the measurement of the activity and length changes of specific muscles during normal locomotion.

Recent advances in technology have enabled a more complete picture of *in vivo* muscle function to be developed. Sonomicrometry techniques, have enabled *in vivo* muscle fascicle length trajectories to be recorded in a number of species and skeletal muscles under a variety of locomotor conditions (e.g. Biewener et al., 1998; Biewener et al., 2004; Carroll, 2004; Daley and Biewener, 2003; Donley et al., 2005; Gillis and Biewener, 2001; Gillis and Biewener, 2002; Higham et al., 2008; Hoffer et al., 1989; Sanford and Wainwright, 2002; Wakeling and Johnston, 1999). An important finding of these reports is that the mechanical behaviour of a muscle is not fixed, and can alter in response to changes in locomotor condition. For example, turkey ankle extensor muscles undergo much greater strains during incline locomotion than during locomotion on the flat (Gabaldon et al., 2004; Roberts et al., 1997). In addition, muscles are also able to adapt their mechanical work output, in response to changes in locomotor conditions, by changing the timing of myoelectric activity in relation to force production (Daley and Biewener, 2003; Gabaldon et al., 2004).

There is a wide range of information available on the contractile and physiological properties of rat muscles (Armstrong and Phelps, 1984; Close, 1964; Close and Luff, 1974; Delp and Duan, 1996; Schiaffino and Reggiani, 1996), and this model is commonly used in a wide range of physiological studies. Despite this, *in vivo* muscle fascicle behaviour of rat muscle during locomotion has only been documented in two reports, both focusing on proximal hind limb muscles: biceps femoris and vastus lateralis (Gillis and Biewener, 2001; Gillis and Biewener, 2002). The soleus, plantaris and medial gastrocnemius muscles in the rat have distinctly different fibre type populations (Armstrong and Phelps, 1984; Delp and Duan, 1996) and therefore provide a useful example with which to investigate how different fibre type populations adapt their mechanical work and power output through changes in mechanical behaviour (fascicle strain and strain rates) and/or activation timing in relation to force production. We present the first report of *in vivo* muscle fascicle strain and strain rates for rat ankle extensor muscles during treadmill locomotion at a range of velocity/incline combinations. These data represent a valuable opportunity to investigate how systematic changes in locomotor velocity and incline influence *in vivo* muscle

fascicle behaviour in a group of anatomically synergistic muscles, with distinctly different mechanical properties and fibre type populations. As rat muscle has been used extensively in studies of muscle physiology and mechanics, it is of value to quantify the *in vivo* conditions under which these tissues function. We therefore also investigate the influence of muscle fascicle mechanical properties, myoelectric intensity, activation timing and duration and muscle fascicle strain and strain rate on the potential for force and power production during locomotion using a simple muscle model. Detailed reports of myoelectric data and some measurements of fascicle strains and strain rates have been reported elsewhere (Hodson-Tole and Wakeling, 2007; Hodson-Tole and Wakeling, 2008a; Hodson-Tole and Wakeling, 2008b).

MATERIALS AND METHODS

Subjects

Myoelectric and sonomicrometric data were collected from the soleus, plantaris and medial gastrocnemius muscles of the right hind limb of 19 female Sprague Dawley rats [approximate age 5–6 months; mass 250.07±18.57 g (mean±s.d.)]. The rats were housed in pairs in cages, maintained on standard rat feed and kept in a temperature-controlled room (20°C) with a 12 h:12 h light:dark cycle. All rats had undergone a five week training programme during which time they were acclimatised to run on a custom-built, motorised treadmill at nine speed (20–50 cm s^{-1}) and incline (0–25 deg.) combinations. All procedures were conducted in accordance with current UK Home Office regulations.

Surgical procedures

Surgical and data collection procedures have previously been described elsewhere (Hodson-Tole and Wakeling, 2007). Rats received a subcutaneous injection of atropine (0.01 mg kg^{-1}) and were anaesthetised using halothane gas (4% induction; 1.75–2% maintenance). The right hind limb and an area on the back over and just caudal to the scapulae were shaved, scrubbed (4% chlorhexidine gluconate solution, E-Z Scrub, Becton, Dickinson and Co., Franklin Lakes, NJ, USA) and painted with a povidone iodine solution. Two incisions were made, one caudal to the scapulae and the second along the lateral aspect of the right hind limb approximately parallel to the tibia. To keep the wires from the implanted transducers secure during the post-operative recovery period and during data collection they were fed through a subcutaneous tunnel, which was created between the two incisions, so that excess wires were externalised in the region of the scapulae and the transducers were situated in the region of the muscles of interest. No signs of discomfort relating to this procedure were observed post-operatively in any of the subjects.

Offset twist-hook bipolar silver-wire electrodes (0.1 mm diameter, California Fine Wire Inc., Grover Beach, CA, USA), with tips bared of 0.5 mm of insulation, were surgically implanted into two of the muscles of interest using fine tip forceps. Approximately 2 mm separated the electrode tips in each muscle. They were placed, at a depth of approximately 3 mm, in the mid-belly region of the soleus and plantaris muscles and in the medio-caudal region of the medial gastrocnemius as this area has been identified as containing predominantly fast, myosin heavy chain type IIB fibres (Armstrong and Phelps, 1984; Delp and Duan, 1996). In addition, two sonomicrometry crystals (1.0 mm+38 gauge stainless steel lead wires, Sonometrics, London, ON, Canada) were implanted into the third muscle of interest, following the orientation of the muscle fascicles as closely as possible (see Table 1 for details of data collected from each subject). Fascicle length changes can be tracked with greater than 95% accuracy if alignment of crystals is less than 18 deg. from the alignment of the fascicle. We are confident that our crystal alignment fell within this boundary; however, it should be noted that any changes in pennation angle during contraction due to fibre rotation are not accounted for here and are likely to cause some overestimation of fascicle strain.

Table 1. Details of data set collected and presented from ankle extensor muscles of each subject [medial gastrocnemius (MG), plantaris (PL) and soleus (SL)]

	Myoelectric data			Sonomicrometry data		
Subject	MG	PL	SL	MG	PL	SL
1	X	X				X
2		X				X
3	X		X		X	
4	X		X		X	
5			X		X	
6	X				X	
7			X	X		
8		X	X	X		
9			X	X		
10		X		X		
11	X	X				
12	X	X				X
13					X	
14					X	
15						X
16				X		
17				X		
18						X
19						X

To ensure that each animal had full range of movement of the limb, slack wire from both types of transducer was fed under the skin in the area surrounding the hip. Excess wire in the region of the scapulae was placed into a small cotton pouch that was secured under a small jacket, fashioned for each subject from elasticised bandage (Vetwrap™, 3M United Kingdom PLC, Bracknell, UK). The jacket protected the surgical incision, secured the wires and enabled the animals to be housed in pairs post-operatively. The two incisions were sutured shut with 5-0 vicryl suture and animals received post-operative analgesia (buprenorphine, 0.01 mg kg^{-1}, subcutaneously) during the 48 h recovery period.

Data collection

All data were collected 48 h post surgery in an electrically shielded room. Each rat ran a three block, randomised exercise protocol incorporating nine speed/incline conditions (0 deg. at 20, 30, 40 and 50 cm s^{-1}; 10 deg. at 20, 30 and 40 cm s^{-1}; 20 deg. and 25 deg. at 20 cm s^{-1}). During each trial the position of the right hind limb was recorded using two cameras (100 Hz, A602f, Basler, Ahrensberg, Germany) connected to the data collection computer *via* IEEE 1394 ports. Myoelectric signals were amplified and band-pass filtered (30–1000 Hz, CP511 A.C. amplifier, Astro-Med. Inc., West Warwick, RI, USA) and collected (3200 Hz) through a 16-bit data acquisition card (PCI-6221, National Instruments Corps., Austin, TX, USA). Sonomicrometry signals were collected (715 Hz) using sonometrics systems hardware, relayed to the data collection computer *via* an analog–digital converter. All systems were synchronously triggered *via* a 16-bit data acquisition card and data collected for periods of 30 s. On completion of the trial animals were euthanased with an intraperitoneal overdose of pentobarbitone, and dissection carried out to confirm the location of the fine-wire electrodes and sonomicrometric crystals in each of the muscles.

Table 2. Total number of strides analysed for the determination of muscle fibre strain and strain rate

	Muscle		
Condition	m. gastrocnemius	soleus	plantaris
0 deg. 20 cm s^{-1}	285	219	280
0 deg. 30 cm s^{-1}	322	291	403
0 deg. 40 cm s^{-1}	139	96	186
0 deg. 50 cm s^{-1}	277	104	229
10 deg. 20 cm s^{-1}	183	135	126
10 deg. 30 cm s^{-1}	320	202	292
10 deg. 40 cm s^{-1}	265	87	154
20 deg. 20 cm s^{-1}	91	129	192
25 deg. 20 cm s^{-1}	153	112	190
Total number of strides	2035	1375	2052

Determination of muscle fascicle strain and strain rates

Sonomicrometry data were used to determine muscle fascicle strain and strain rates. Video data were used to define the timing of successive footfalls of the right hind limb of each subject during each trial. These times were used to partition sonomicrometry signals into complete strides (Table 2). Within each subject, traces for each condition were grouped and, based on least squares minimisation, a three harmonic Fourier series:

$$L = \frac{\mathrm{s}}{2} + \sum_{h=1}^{3} \mathrm{c}_h \sin(\mathrm{o}_h + hj) \ , \quad (1)$$

was fitted to the measured lengths L, to give a quantifiable curve of best fit, where s and c represent magnitude constants, o indicates a phase constant, h indicates harmonic number and j represents an angle within the gait cycle. Muscle fascicle strain (ε) was calculated as:

$$\varepsilon = \frac{L - L_\mathrm{o}}{L_\mathrm{o}} \ , \quad (2)$$

where L_o was the resting length defined as the mean of the maximum and minimum lengths recorded in each stride (Gabaldon et al., 2004). Ideally, L_o should be defined as the muscle length at the mid-point of the stress–strain (σ–ε) plateau. The stress–strain relationship was however not defined in the work presented here. If L_o was too high muscle fascicle strains and strain rates would be underestimates, if L_o was too low values would be overestimates. Other workers have defined L_o based on strains measured in subjects during quiet standing (Biewener and Baudinette, 1995; Daley and Biewener, 2003). Rats however adopt a more crouched posture with a large amount of ankle and knee flexion during quiet standing compared with during locomotion. Defining L_o based on resting measurements would therefore significantly underestimate measurements compared with the value for L_o used.

Muscle fascicle strain rate ($\dot{\varepsilon}$) was determined as:

$$\dot{\varepsilon} = \frac{\mathrm{d}}{\mathrm{d}t}(\varepsilon) \ , \quad (3)$$

where t defines time. Negative values for muscle fascicle strain rate represented fascicle shortening whereas positive values represented fascicle lengthening.

For each subject and condition mean measurements of strain, shortening strain (negative strain values), lengthening strain (positive strain values), peak-to-peak strain, shortening strain rate and lengthening strain rate were made for the complete stride from the Fourier series. Data from the soleus during the fastest conditions (0 deg. 40 cm s^{-1} and 0 deg. 50 cm s^{-1} and 10 deg. 40 cm s^{-1}) were only successfully collected from one subject, so plots of these data only show mean values and do not include values for s.e.m.

Determination of myoelectric intensity, duty cycle and phase delay

Myoelectric data were analysed using wavelet transformation as previously described (Hodson-Tole and Wakeling, 2007). Briefly, a filter bank of 20 non-linearly scaled wavelets, $0 \le k \le 19$, was used to resolve the myoelectric signals into time–frequency space (von Tscharner, 2000). Due to the quantity of low frequency (<100 Hz) noise identified in the signal the first four wavelet domains ($0 \le k \le 3$) were excluded from further analysis, and the remaining frequency band that was analysed ($4 \le k \le 19$) covered the frequencies from 69.92 Hz to 1325.00 Hz. The intensity, i, of the signal at each wavelet domain was then calculated at each time point from the magnitude and the first-time derivative of the square of the convoluted signal. Mean intensities were calculated for strides collected during each locomotor condition.

To calculate the duration of myoelectric activity, and hence the myoelectric duty cycle, a threshold intensity was defined whereby values greater than the threshold were considered to represent myoelectric activity and values below the threshold were considered to represent times when the muscle was inactive. The thresholds were defined as twice the lowest mean level of intensity, calculated in all conditions from the period of minimum myoelectric activity (approximately 60–80% stride duration). Thresholds were calculated per individual and used to define periods of myoelectric activity within each subject before mean values were calculated for each locomotor condition. Myoelectric duty cycle was defined as the proportion of the stride duration that myoelectric activity above the defined threshold was recorded.

Two phase delay times were calculated: (1) activation phase – the time between the beginning of myoelectric activity and the time of maximum muscle fascicle strain. A positive value represented myoelectric activity beginning after maximum strain had occurred whereas a negative value represented myoelectric activity beginning before maximum strain had occurred. (2) Deactivation phase – the time between the end of myoelectric activity and the minimum muscle fascicle strain value. A negative value represented myoelectric activity ceasing before the minimum muscle fascicle strain occurred whereas a positive value represented the minimum strain value occurring before myoelectric activity had stopped.

As myoelectric and sonomicrometric measurements for each muscle were not recorded simultaneously within each individual (Table 1) it was not possible to calculate these values per subject. The calculations were therefore based on the mean muscle fascicle strain measurements and mean myoelectric on/off time values calculated for each muscle under each condition. Standard error values were therefore not calculated for these data.

Muscle model

To determine the effect of activation phase and level of activation on total force, F, and mechanical power, P, production a simple Hill-based muscle model was built:

$$F = a(t) \times \sigma(\varepsilon) \times \sigma(\dot{\varepsilon}) \ , \quad (4)$$

where a is normalised activation and σ is normalised stress. From Eqn 4 F is a normalised value, with actual muscle force being the product of F and the muscle's cross-sectional area (A) and maximal isometric stress (σ_o).

Activation was defined by a first-order differential equation (Zajac, 1989):

$$\frac{\mathrm{d}}{\mathrm{d}t}(a)+\left[\frac{1}{\tau_{act}}.(\beta+[1-\beta]u(t))\right].a(t)=\left(\frac{1}{\tau_{act}}\right).u(t)\ , \quad (5)$$

which modelled the net result of excitation–contraction coupling, acting as a low pass filter and introducing a delay between neural excitation, u, and the muscle's active state. The ratio (β) between activation (τ_{act}) and deactivation rate constants was defined as 0.5 (Zajac, 1989).

The active stress–strain properties were defined as:

$$\sigma(\varepsilon)=e^{-\left|\frac{L/L_o^{\ w}-1}{s}\right|^r}\ , \quad (6)$$

where r determines roundness, w determines skewness and s determines width of the stress–strain relationship (Otten, 1985) (Fig. 1A). In the present study, these values were based on those previously reported for rat muscle (r=2.5, w=2.0, s=0.8) (Otten, 1987). The plateau region of the stress–strain relationship [$\sigma(\varepsilon=0)$] was set to 1 (Fig. 1A). Parallel elastic elements were ignored in the model as they have been shown to play a minor role in force production over the muscle fascicle strains considered here (0.05 and 0.15) (van Leeuwen, 1992). In addition, this model considered muscle fascicles and not the whole muscle, therefore any myofilament or cross-bridge elasticity was assumed to be accounted for by the contractile element active properties (Epstein and Herzog, 1995).

The stress–strain rate properties of both slow and fast fibres were defined by:

$$\sigma(\dot{\varepsilon})=\frac{(1-\dot{\varepsilon}/\dot{\varepsilon}_o)}{1+\dot{\varepsilon}/m\dot{\varepsilon}_o}\ ;\ \dot{\varepsilon}\geq 0\ , \quad (7a)$$

$$\sigma(\dot{\varepsilon})=1.5-0.5\frac{(1+\dot{\varepsilon}/\dot{\varepsilon}_o)}{1-7.56\dot{\varepsilon}/m\dot{\varepsilon}_o}\ ;\ \dot{\varepsilon}<0\ , \quad (7b)$$

$\dot{\varepsilon}_o$ represented maximum unloaded shortening velocity (Aubert, 1956; Hill, 1938) with m=0.25 and $\dot{\varepsilon}_o$=16.30 s^{-1} used for the fast

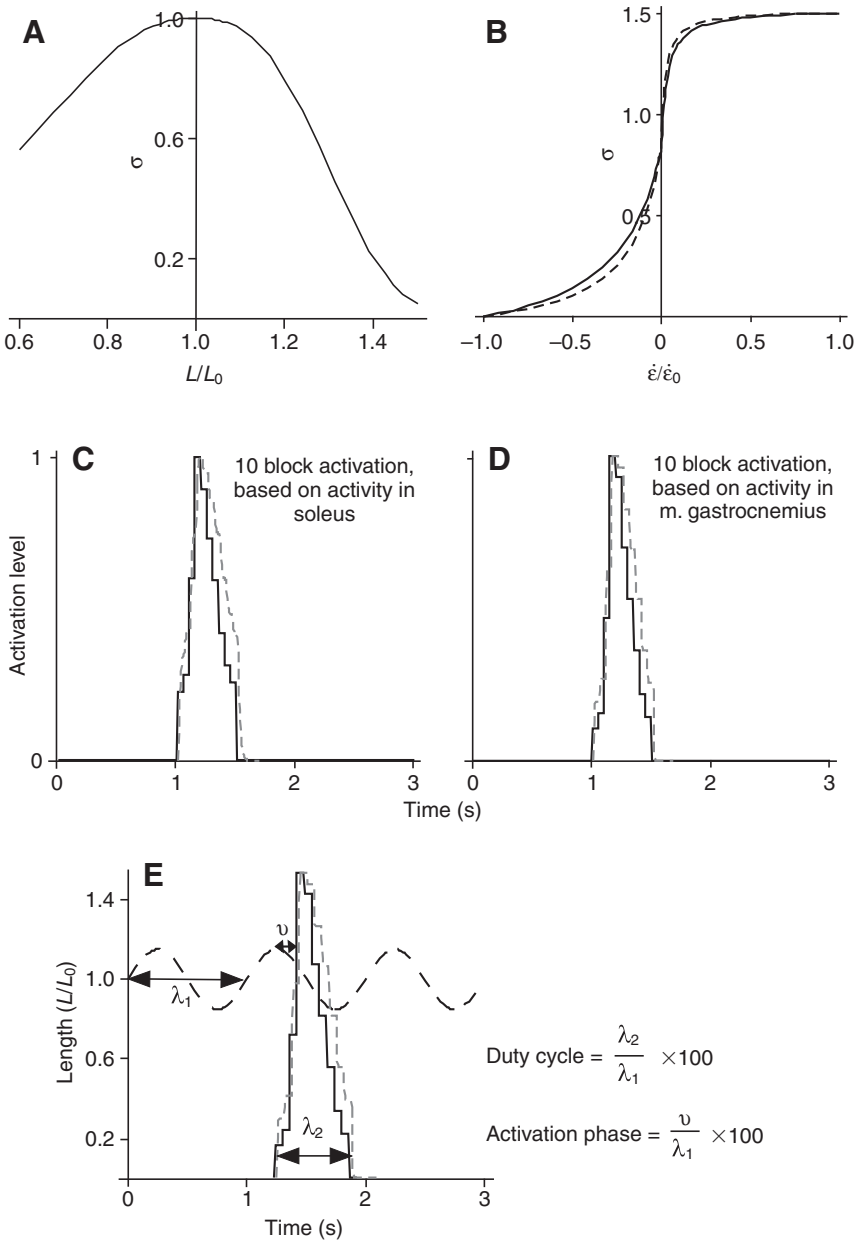

Fig. 1. Properties of a simple Hill based muscle model (A) stress–strain properties, normalized to resting length; (B) stress–strain rate properties for a fast (black solid line) and slow (black broken line) muscle fibre, normalised to maximum shortening strain rate; (C) 10-block activation stimulus based on mean intensity values from the soleus muscle (black solid line) and corresponding muscle activation (grey broken line) with slow activation rates; (D) 10 phase activation stimulus based on mean intensity values from the medial gastrocnemius muscle (black solid line) and corresponding muscle activation (grey broken line) with fast activation rates; (E) 1 Hz strain cycle (black broken line) with activation stimulus overlaid to illustrate duty cycle and activation phase. λ_1 is the stride cycle duration; λ_2 is the duration of activity; and υ is the time between peak length and activation.

fibres and m=0.17 and $\dot{\varepsilon}_o$=5.21 s^{-1} used for the slow fibres (Fig. 1B). Values for m were taken from Otten (Otten, 1987). For slow fibres, $\dot{\varepsilon}_o$ was calculated from reported values from the soleus muscle (2.97 muscle lengths s^{-1} at 35°C) (Caiozzo et al., 1992), divided by the ratio between fibre length and muscle belly length (0.57) (Woittiez et al., 1985), to give fibre lengths per second. For fast fibres, 16.30 s^{-1} has been recorded in the proximal compartment of the medial gastrocnemius muscle at 36°C (De Ruiter et al., 1995). The stress–strain rate values were normalised so that, for isometric contractions, $\sigma(\dot{\varepsilon}_o=0)=1$ (Fig. 1B).

Initial analysis of sonomicrometric data showed that the peak-to-peak strain in medial gastrocnemius was approximately 0.3, while in the soleus and plantaris muscles it was approximately 0.1. In order to reflect these in the model, two 1 Hz sinusoidal strain cycles were modelled with peak-to-peak strains of 0.1 and 0.3. Two 10-block activation patterns were defined, where $u(t)$ was related to the mean myoelectric intensities recorded in the soleus and medial gastrocnemius muscles at 10 evenly spaced time windows, with the appropriate fast and slow τ_{act} (Fig. 1C,D). The effect of activation phase (0–100%) and duty cycle (0–100%) on total force and mechanical power production was then determined, with mechanical power output being a normalised value calculated as product of F and $\Delta\dot{\varepsilon}$ per cycle.

Statistical analysis

Initially, general linear model, full factorial analyses of variance (ANOVAs) were used to determine if significant differences in muscle fascicle strain, muscle fascicle strain rate or myoelectric intensity differed between muscles (SPSS® version 14.0, SPSS, Chicago, IL, USA). In these analyses muscle and condition were defined as fixed factors and subject defined as a random factor. Within each muscle significant differences in strain, strain rate and myoelectric measurements between conditions were also calculated using general linear model ANOVA. In these analyses condition was defined as a fixed factor and subject defined as a random factor. After all tests, when a factor was identified as significant ($P\leq0.05$) *post hoc* Bonferroni tests were applied to identify the location of the significant differences. Results are reported as means±s.e.m.

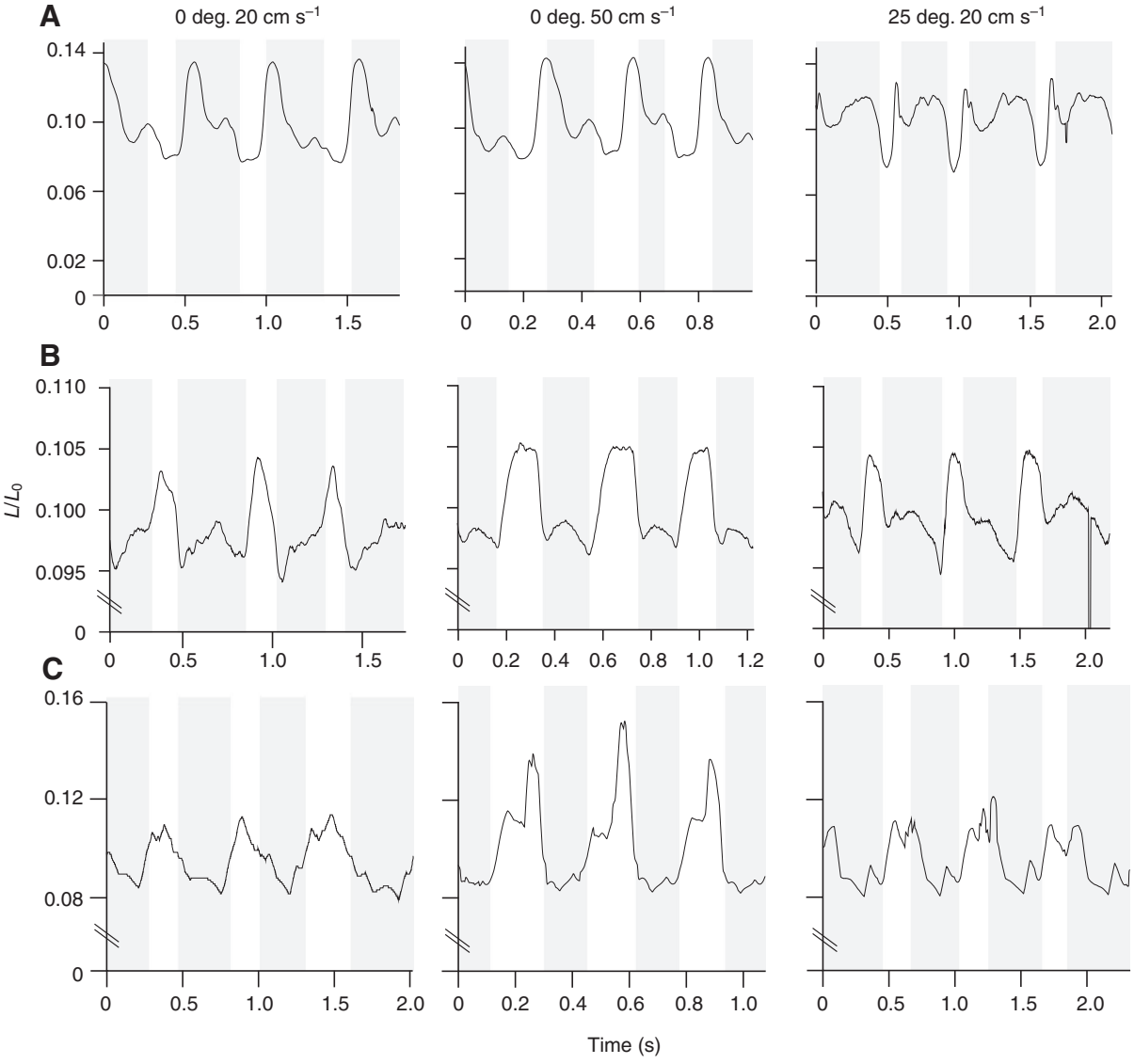

Fig. 2. Example sonomicrography traces from medial gastrocnemius (A), plantaris (B) and soleus (C) from each of the locomotor conditions tested (columns). Grey shading indicates stance phases of each of the four strides shown.

RESULTS

Muscle fascicle strain and strain rate measurements

In each condition each muscle went through a series of stretch-shortening strain cycles, which differed between muscles (Figs 2–5) and were highlighted by differences in the peak-to-peak strains recorded (Fig. 6A). Both the soleus and plantaris had very low peak-to-peak strains ($\Delta\varepsilon<0.1$) in all conditions, while larger values were recorded in the medial gastrocnemius ($\Delta\varepsilon>0.2$). This was reflected in the statistical analysis where peak-to-peak values in the medial gastrocnemius muscle were significantly larger than in either the soleus or plantaris muscles ($P<0.01$, both cases). Within each muscle there were no significant differences in the peak-to-peak strain, minimum strain, maximum strain or the timing of these variables between conditions.

Mean shortening and mean lengthening muscle fascicle strain rates differed significantly between muscles ($P<0.001$, all cases). Significantly greater shortening and lengthening strain rates were recorded in the medial gastrocnemius muscle compared with the soleus and plantaris ($P<0.001$, all cases) (Fig. 6B,C). In the plantaris muscle there were significant differences in both the mean shortening ($P=0.023$) and the mean lengthening ($P=0.002$) strain rates. At 0 deg. 40 cm s^{-1} and 0 deg. 50 cm s^{-1} and 10 deg. 40 cm s^{-1} mean lengthening strain rates were significantly greater than all the other conditions ($P\leq0.032$, all cases). A similar trend was seen in mean shortening strain rates from the plantaris, where significantly faster mean shortening velocities were recorded at faster locomotor velocities (0 deg. 40 cm s^{-1} and 0 deg. 50 cm s^{-1} and 10 deg. 40 cm s^{-1}) compared with the slower locomotor velocities ($P\leq0.032$). In the soleus muscle, there were no significant differences in mean shortening ($P=0.590$) or mean lengthening ($P=0.163$) strain rate values. A similar result was found in the medial gastrocnemius muscle where again no significant differences existed in mean shortening strain rates ($P=0.343$) or mean lengthening strain rates ($P=0.092$).

Myoelectric duty cycle

There were no significant differences in myoelectric duty cycle between muscles ($P=0.092$), although there was a trend for longer duty cycles to occur in the soleus muscle compared with the plantaris

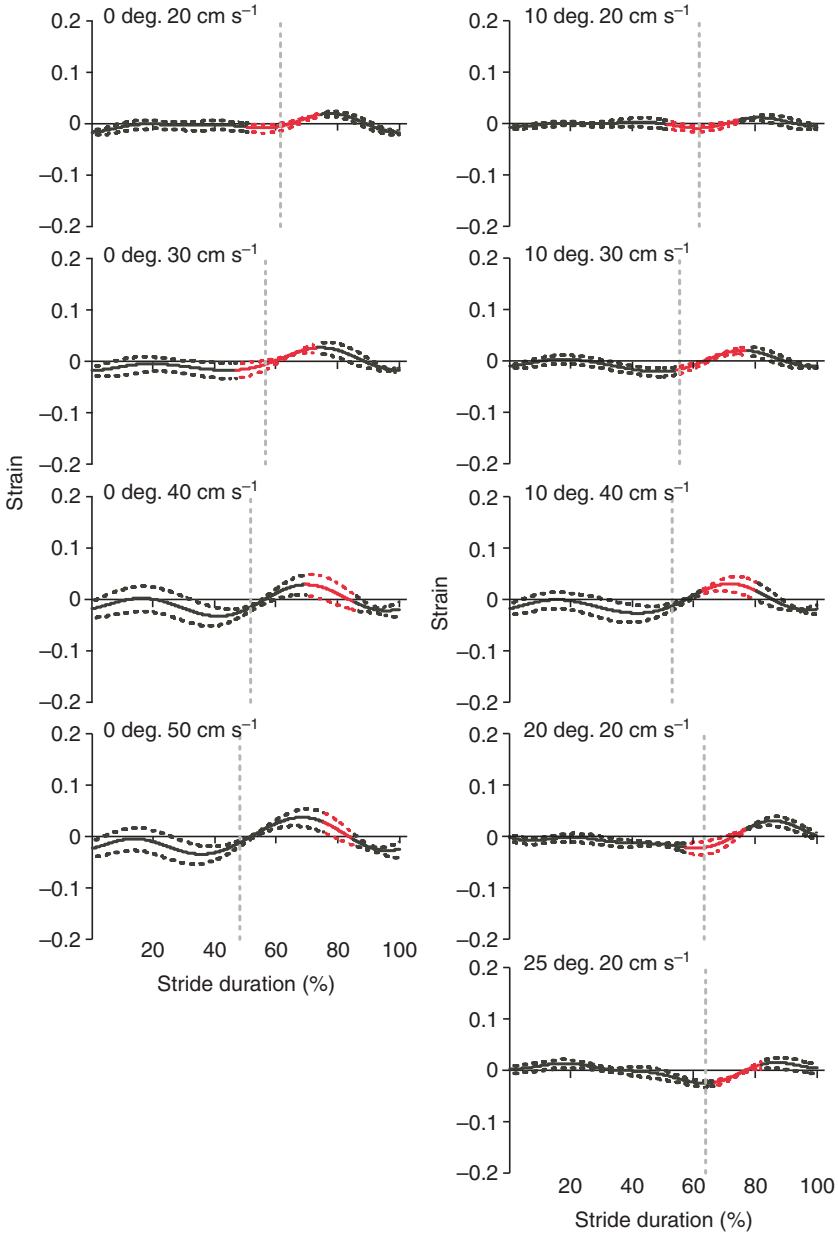

Fig. 3. Muscle fascicle strain as a function of stride duration in the plantaris muscle during each of the locomotor conditions studied. Values are means±s.e.m. (solid and broken line, respectively). Black represents myoelectric activity and red represents no myoelectric activity. Foot off is marked by the grey, broken vertical line.

or medial gastrocnemius (Fig. 7). In the plantaris muscle, myoelectric duty cycle varied significantly between conditions (P=0.002). Differences were significant between 0 deg. 20 cm s^{-1} and both 0 deg. 40 cm s^{-1} and 0 deg. 50 cm s^{-1}, as well as between 0 deg. 30 cm s^{-1} and 0 deg. 40 cm s^{-1} (P≤0.039, all cases). Significant differences between conditions were also identified in the soleus muscle (P=0.030), where both 0 deg. 20 cm s^{-1} and 0 deg. 30 cm s^{-1} differed significantly to 0 deg. 50 cm s^{-1} and 10 deg. 40 cm s^{-1} (P≤0.006 all cases). In addition, a significant difference existed between 0 deg. 40 cm s^{-1} and 0 deg. 50 cm s^{-1} (P=0.028). A significant difference in myoelectric duty cycle was also found in the medial gastrocnemius muscle (P=0.021), with the difference existing between 0 deg. 30 cm s^{-1} and 0 deg. 50 cm s^{-1}. In all muscles there was a trend for longer duty cycles to occur at faster velocities, with no differences seen between conditions with similar velocities but different inclines.

Myoelectric activation and deactivation phase relations

Two myoelectric phases were calculated for each muscle and condition. Initially, the activation phase relation, occurring between the beginning of myoelectric activity and the time of maximum muscle fascicle strain, was calculated (Fig. 8A). Values in the plantaris muscle were positive, indicating that myoelectric activity began after maximum strain had occurred, in all conditions when velocity >20 cm s^{-1}. When locomotor velocity was 20 cm s^{-1} (0 deg., 10 deg., 20 deg., 25 deg.), values were negative, indicating that myoelectric activity began before maximum strain had occurred. In the soleus muscle, myoelectric activity began after maximum strain had occurred in all conditions except 10 deg. 40 cm s^{-1}, where activity began before the time of maximum strain (Fig. 8A). In the medial gastrocnemius muscle, myoelectric activity began before maximum strain had occurred in all conditions except 0 deg. 40 cm s^{-1} where maximum strain occurred before myoelectric activity had begun (Fig. 8A).

The second phase duration to be calculated was the deactivation phase, which was the time between the end of myoelectric activity and the minimum strain value (Fig. 8B). In the plantaris muscle values were positive, indicating that myoelectric activity had ended after minimum muscle fascicle strain occurred, in all conditions except

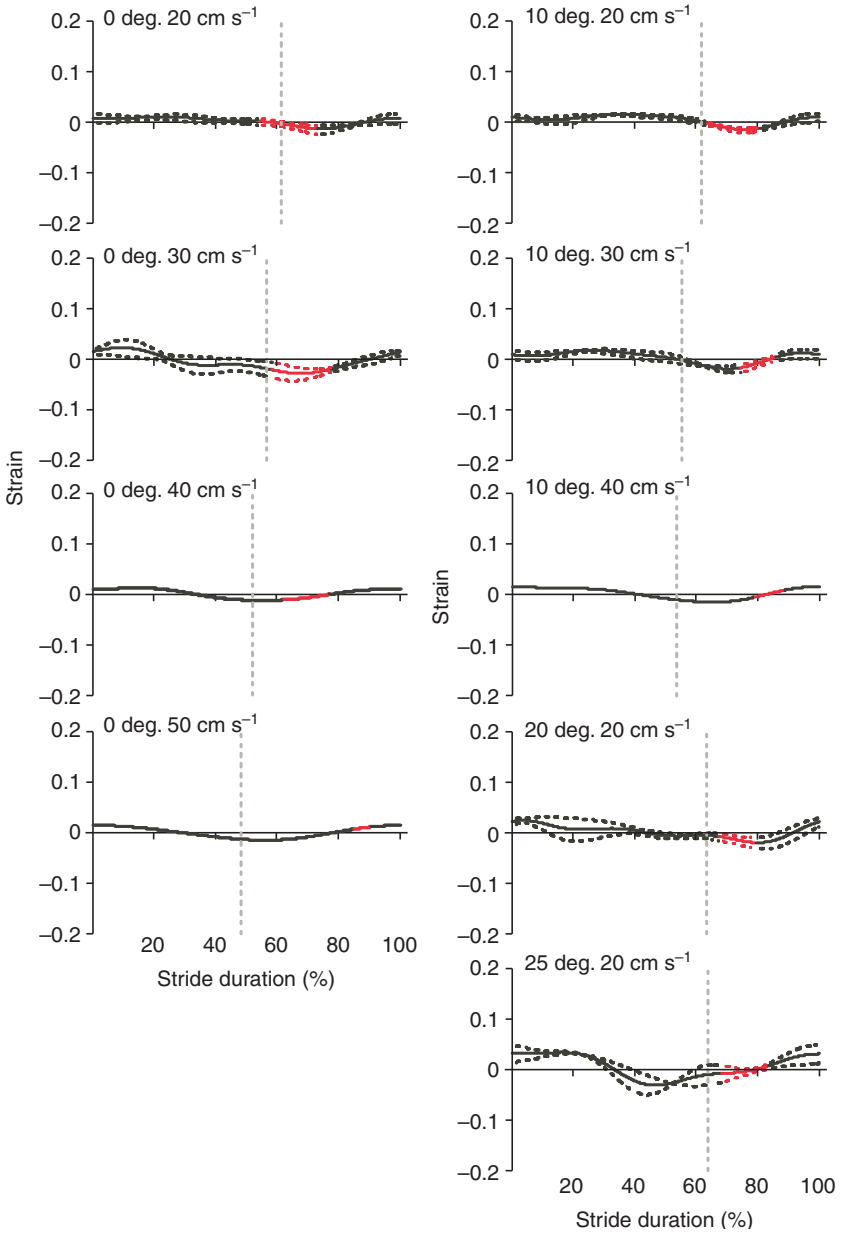

Fig. 4. Muscle fascicle strain as a function of stride duration in the soleus muscle during each of the locomotor conditions studied. Values are means±s.e.m. (solid and broken line, respectively). Black represents myoelectric activity and red represents no myoelectric activity. Foot off is marked by the grey, broken vertical line.

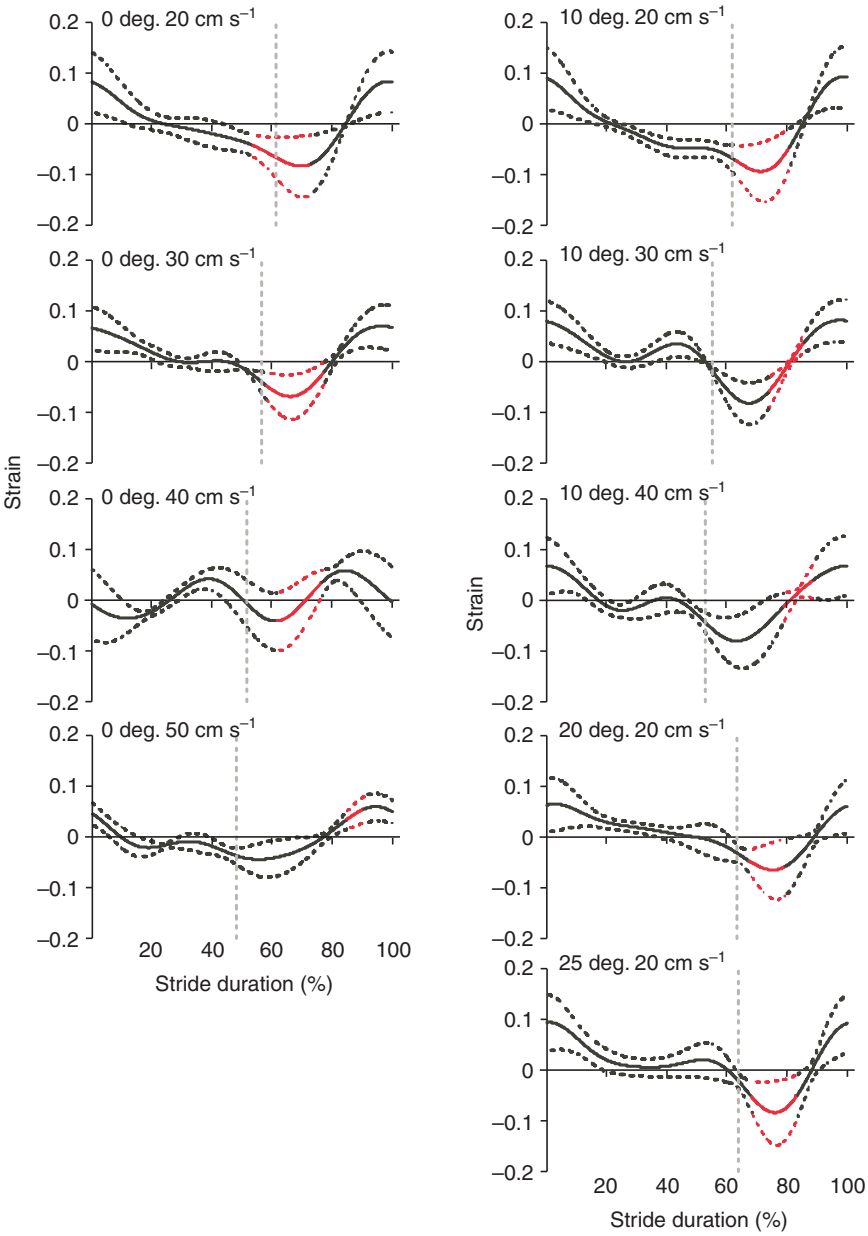

Fig. 5. Muscle fascicle strain as a function of stride duration in the medial gastrocnemius muscle during each of the locomotor conditions studied. Values are means±s.e.m. (solid and broken line, respectively). Black represents myoelectric activity and red represents no myoelectric activity. Foot off is marked by the grey, broken vertical line.

those with a velocity of 20 cm s^{-1}. In the soleus muscle, myoelectric activity ended before the minimum muscle fascicle strain had occurred during the slowest conditions, except 25 deg. 20 cm s^{-1}. The time between the end of activity and minimum strain became less as locomotor velocity increased until, at locomotor velocity >40 cm s^{-1}, myoelectric activity ended after the minimum strain value had occurred. A similar trend was seen in the medial gastrocnemius muscle where, at locomotor velocities <40 cm s^{-1}, myoelectric activity ended before minimum muscle fascicle strain occurred. At locomotor velocities of 40 cm s^{-1} and faster minimum muscle fascicle strain occurred during the period of myoelectric activity.

Modelled effects of duty cycle and activation phase

The effects of activation phase (time between onset of myoelectric activity and maximum strain value) and duty cycle (duration of myoelectric activity as a proportion of stride duration) and activation pattern on total force and mechanical power production were calculated using a simple muscle model. In all simulations the highest total forces were predicted at the higher duty cycles (>50%). At higher strain amplitudes, maximum total force was only predicted when the activation phase was >25% or duty cycle was >75%. Duty cycle and activation phase had less influence on the total force produced when strain amplitude was low (0.1 peak-to-peak) and activation followed the 10-block pattern related to myoelectric activity in the soleus (Fig. 9).

Distinctive differences in total mechanical power output were apparent between simulations (Fig. 10). In all scenarios greater positive and negative values were recorded under high strain conditions (0.3 peak-to-peak). In general, when duty cycle <75% negative power occurred when activation phase was between –25% and +25%, and positive power occurred when activation phase was greater than 25%. At higher duty cycles (>75%), positive power occurred when activation phase was >0%. Differences in contour plots were subtle between the fast and slow models (Fig. 10), indicating that activation pattern and strain were more influential on mechanical power production than the individual fibre properties.

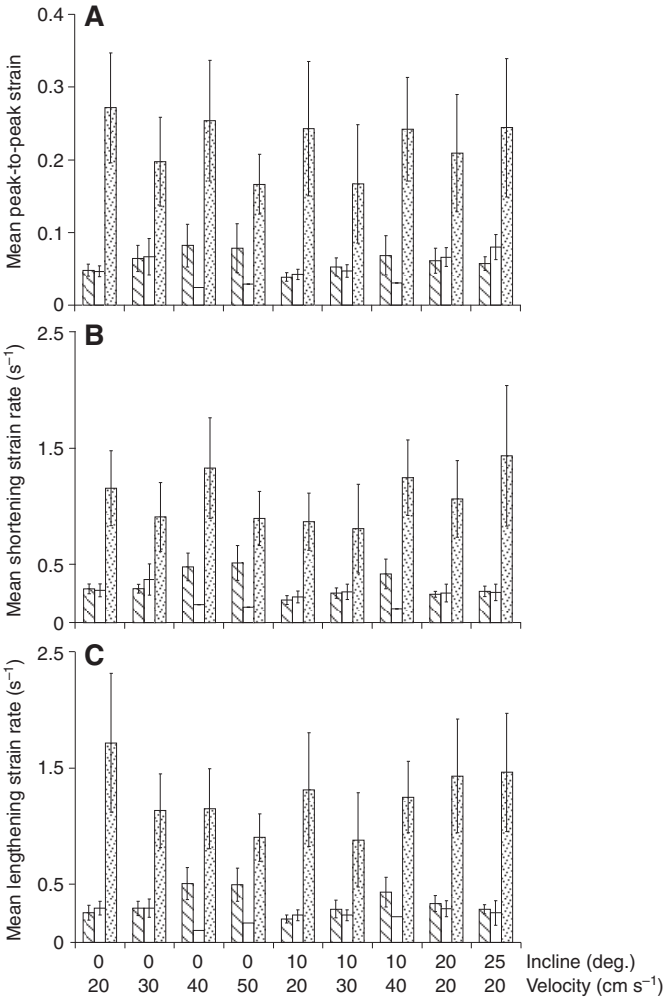

Fig. 6. (A) Mean peak-to-peak strain values; (B) mean muscle fascicle shortening strain rate; (C) muscle fascicle lengthening strain rate recorded in each locomotor condition for the plantaris (diagonal stripes), soleus (no fill) and medial gastrocnemius (speckled). Values are means±s.e.m. with incline (deg.) and velocity (cm s^{-1}).

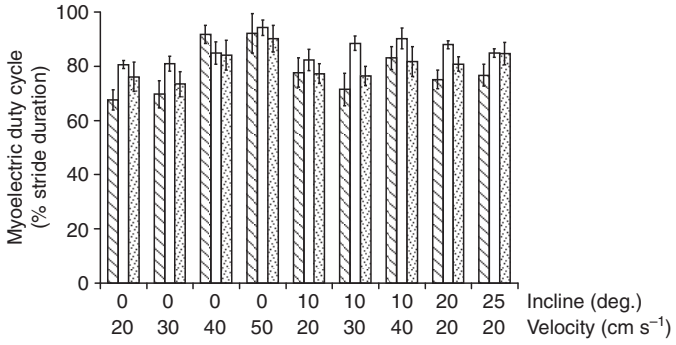

Fig. 7. Myoelectric duty cycle for the plantaris (diagonal stripes), soleus (no fill) and medial gastrocnemius (speckled) muscles in each of the locomotor conditions. Values are means±s.e.m. with incline (deg.) and velocity (cm s^{-1}).

DISCUSSION

Mechanical behaviour and activation of the three ankle extensor muscles

The three muscles investigated have been documented as having distinctly different morphology and fibre type populations (Armstrong and Phelps, 1984; Delp and Duan, 1996) and intrinsic properties (Caiozzo et al., 1992; De Ruiter et al., 1995; Norenberg and Fitts, 2004; Swoap et al., 1997). Data presented here may therefore be considered to represent *in vivo* behaviour of three distinct fibre type populations, with soleus representing a population of slower fibre types, medial gastrocnemius representing a population of predominantly faster fibre types and plantaris representing a mixed population of fibre types. The measurements of *in vivo* muscle fascicle strains and strain rates presented provide some insight into the behaviour and function of these muscles and hence these fibre type populations, during normal locomotion, which have not been previously reported.

The plantaris and medial gastrocnemius muscles both span the knee and ankle joints whereas the soleus muscle only crosses the ankle joint. It is therefore surprising to find that the *in vivo* behaviour of the plantaris was more similar to the soleus than to the behaviour of the medial gastrocnemius. Peak-to-peak strains in both the soleus and plantaris were low (<0.1) (Fig. 6A), indicating that both of these muscles worked close to isometrically in all conditions. This agrees with previous work in other animal species (Biewener and Baudinette, 1995; Fukunaga et al., 2001; Griffiths, 1991; Hoffer et al., 1989; Lichtwark and Wilson, 2006; Roberts et al., 1997) and provides further support to the proposed existence of a division of labour between proximal (mechanical work production) and distal (isometric force production) limb muscles (Biewener,

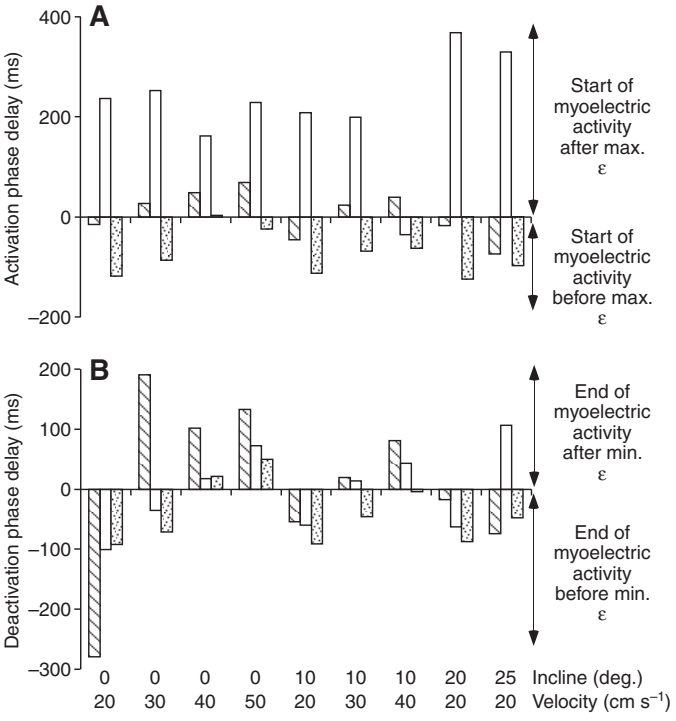

Fig. 8. Mean phase delay times calculated for the plantaris (diagonal stripes), soleus (no fill) and medial gastrocnemius (speckled) muscles during each locomotor condition. (A) Represents activation phase defined as the time between the beginning of myoelectric activity and the time of maximum muscle fascicle strain; (B) represents the deactivation phase defined as the time between the end of myoelectric activity and the minimum muscle fascicle strain value.

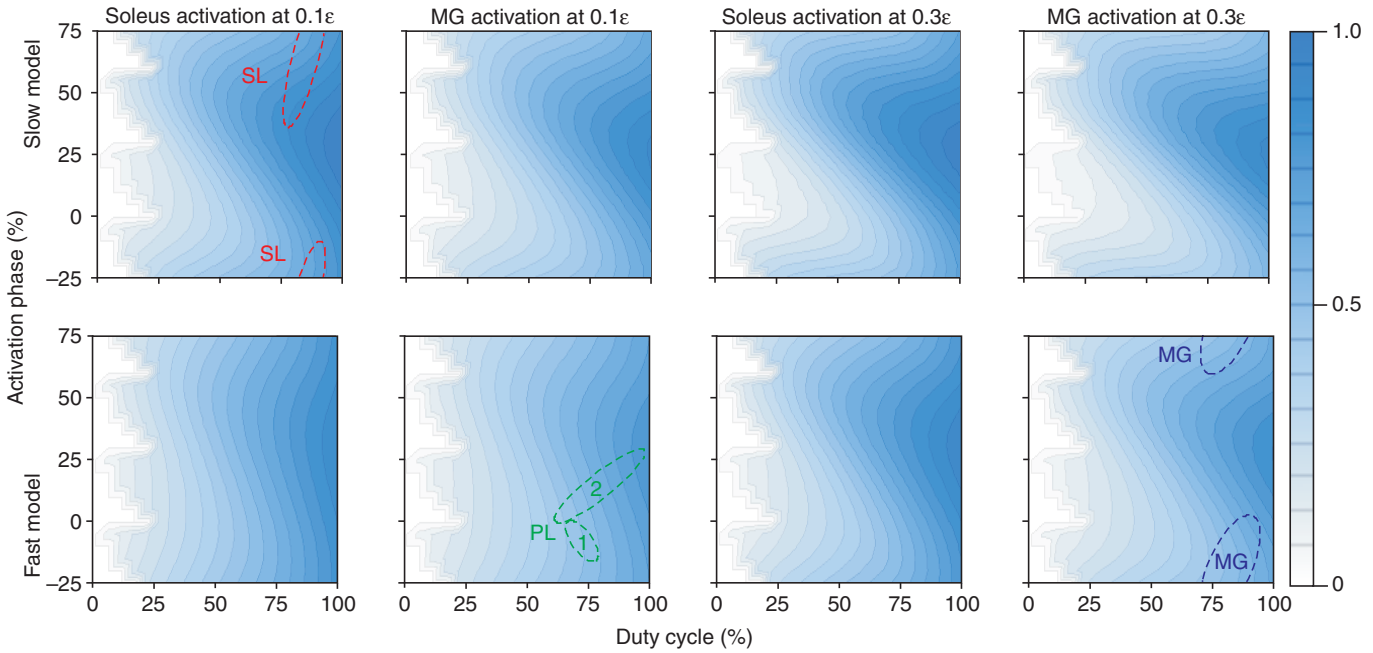

Fig. 9. Total force simulated using two activation and peak-to-peak strain patterns (columns) with slow (top row) and fast (bottom row) muscle models. Regions representing 0.99 quantiles of the activation phases and duty cycles recorded from soleus (SL, red broken line), medial gastrocnemius (MG, blue broken line) and the plantaris at speeds of 20 cm s^{-1} (PL, green broken line, 1) and faster (PL, green broken line, 2) are shown. Values are normalised to the maximum total force value.

1998; Biewener and Roberts, 2000). The similarity between the strains recorded in the soleus and plantaris may be explained by their similar fascicle lengths [18.75±2.42 mm and 22.09±5.47 mm, respectively (Hodson-Tole and Wakeling, 2008a)] especially when compared with the much shorter fascicle lengths reported for medial gastrocnemius [12.23±5.50 mm (Hodson-Tole and Wakeling, 2008a)]. In addition, the plantaris has a slightly shorter moment arm about the knee joint than the medial gastrocnemius [1.90 mm *versus* 2.25 mm (E.F.H.-T., unpublished data)].

The low strains recorded in the soleus and plantaris muscles suggest that they do not act to generate or absorb a large amount of mechanical work or power but instead function to generate high levels of force and/or facilitate elastic energy storage in their associated tendons with small fluctuations in strain. It should also be noted that when a muscle operates at minimal strain rates its force development is very sensitive to changes in strain and thus it is possible that fluctuations in strain rate produce large changes in the force developed by the soleus and plantaris muscles. Generating high forces at low strains can be considered beneficial for two reasons. Firstly, operating at higher shortening velocities and greater power outputs would be energetically more costly (Fenn, 1924). Secondly, the force–velocity relationship of a muscle predicts that it produces greater force during slower contractions (Fig. 1B) (Hill, 1938). A given force can therefore be generated with fewer active fibres at slower muscle fascicle shortening velocities, resulting in a lower metabolic energy cost and an improved economy of locomotion (Gabaldon et al., 2004; Roberts et al., 1997). Although force was not recorded in the current study, the results of the model simulations appear to support this claim, as the activation phase and duty cycles recorded in both the plantaris and soleus correspond to regions where high total force output occurred in the model's results (Fig. 9).

The *in vivo* behaviour of the medial gastrocnemius was noticeably different to the soleus and plantaris muscles. The peak-to-peak strains were much greater and muscle fascicle shortening and lengthening strain rates were much higher than in the other two muscles (Fig. 6B,C). This may be the result of differences in fascicle lengths between the three muscles [12.23±5.5 mm *versus* soleus: 18.75±2.42 and plantaris: 22.09±5.47 mm (Hodson-Tole and Wakeling, 2008a)] or may indicate this muscle operated to generate mechanical power using greater fascicle length changes at faster strain rates. The latter suggestion, however, is contradicted by the results of the model simulations, which suggest that the activation phase and duty cycle values recorded in the medial gastrocnemius would result in negative mechanical power output (Fig. 10).

The fascicle strain and strain rates presented should be considered in light of two factors. Firstly, the medial gastrocnemius has been shown to be composed of two physiologically distinct compartments (De Ruiter et al., 1995). Recordings in the present study were only made in the proximal compartment and therefore no information on the mechanical behaviour or activation patterns within the distal compartments were collected. As the distal compartment has been shown to have fibres with significantly faster maximum shortening strain rates and greater maximum isometric stress values (De Ruiter et al., 1995), it is likely to have a significant influence on the overall force and power producing capability of the muscle. A full picture of the behaviour of the whole medial gastrocnemius muscle and its potential for power generating behaviour is therefore not possible here. Further insight and understanding of muscle mechanics could however be attained by investigating the interaction and co-ordination between physiologically different compartments within a muscle during different locomotor tasks. Secondly, the results presented here will have been influenced by the definition of L_o. The stress–strain relationship was not defined in the work presented, so L_o was defined as the mean of the maximum and minimum lengths recorded in each stride following previously reported methods (Gabaldon et al., 2004). This appeared to be the best approach for the calculation of L_o in the present study. Future work would however benefit from an approach whereby *in vivo* measures of L_o could be defined.

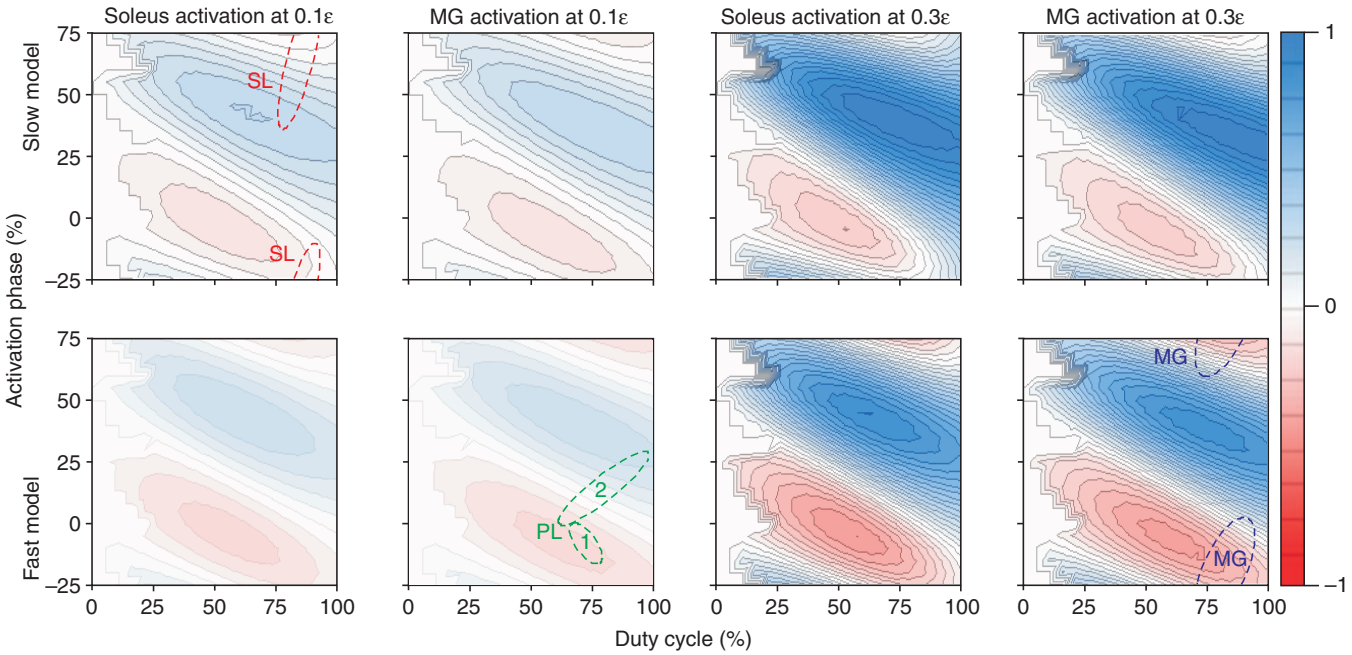

Fig. 10. Mechanical power output simulated using two activation and peak-to-peak strain patterns (columns) with slow (top row) and fast (bottom row) muscle models. Regions representing 0.99 quantiles of the activation phases and duty cycles recorded from soleus (SL, red broken line), medial gastrocnemius (MG, blue broken line) and the plantaris at speeds of 20 cm s^{-1} (PL, green broken line, 1) and faster (PL, green broken line, 2) are shown. Values are normalised to the maximum total force value.

The strain trajectories within each of the muscles were very similar between locomotor conditions (Figs 3–5), indicating that, under the conditions tested here, changes in mechanical force and/or power output are a function of changes in motor control, reflected by variation in activation–deactivation times, myoelectric intensity or motor unit recruitment pattern(s), and not a function of changes in the muscles' strain characteristics. This is in agreement with previous findings in guinea fowl (Daley and Biewener, 2003), and also with data presented here where the soleus and medial gastrocnemius muscles change the deactivation phase in response to changes in velocity (Fig. 8B). The relationship between myoelectric activity and fascicle length trajectories suggest that, under some locomotor conditions, the plantaris and medial gastrocnemius muscles may utilise stretch-activated force enhancement (Edman et al., 1978; Herzog and

Table 3. Percentage variation in the maximum (A) and minimum (B) mechanical power output and maximum total force output (C) predicted by the model when the model was re-run with maximum eccentric force=180% σ_o or L_o=115% L_o

A	Maximum mechanical power output							
	Medial gastrocnemius				Soleus			
Model	Fast		Slow		Fast		Slow	
Strain	0.1	0.3	0.1	0.3	0.1	0.3	0.1	0.3
180% σ_o	100	100	100	100	100	100	100	100
115% L_o	99	98	100	98	98	98	98	98
B	Minimum mechanical power output							
	Medial gastrocnemius				Soleus			
Model	Fast		Slow		Fast		Slow	
Strain	0.1	0.3	0.1	0.3	0.1	0.3	0.1	0.3
180% σ_o	109	115	116	120	109	114	116	119
115% L_o	98	97	98	97	98	97	98	97
C	Maximum total force output							
	Medial gastrocnemius				Soleus			
Model	Fast		Slow		Fast		Slow	
Strain	0.1	0.3	0.1	0.3	0.1	0.3	0.1	0.3
180% σ_o	109	115	117	119	109	115	117	119
115% L_o	99	99	99	100	99	99	99	100

Force (F) was a normalised value calculated from Eqn 4, and power was calculated as the product of F and Δ strain rate per cycle.

Leonard, 2000; Lee and Herzog, 2002) to maximise power output, by activating the muscle while fascicle strain was still increasing (Fig. 8A). In addition, at the slowest locomotor velocity ($20\,cm\,s^{-1}$) the plantaris may show a strategy of minimising mechanical power absorption by ending myoelectric activity before the minimum strain was reached (Fig. 8B). A strategy of minimising power absorption at the onset of muscle activity may be evident in soleus data, as in nearly all conditions myoelectric activity began after maximum strain had occurred (Fig. 8A). Such a strategy would probably limit the amount of force produced during the activation period, due to the muscle's slow activation time. It would, however, go some way to offsetting the negative power output following the end of myoelectric activity when the muscle is unlikely to have enough time to fully relax before lengthening occurs. The results of the model support the suggestion that the soleus acts to reduce the amount of negative power and, at lower duty cycles, positive power values are predicted (Fig. 10). In addition, total force output is optimised with the phase and duty cycles recorded, particularly during the simulation using the activation based on soleus activity (Fig. 9).

Predicted influence of activation phase and duty cycle on force and power output

The simple muscle model presented was used to identify general patterns in the relationship between activation phase and duty cycle on force and power output in examples of slow and fast fibres, subjected to two different strain cycles. In this abstracted form this work is not aimed at identifying intricate details of such relationships. While we are aware that some aspects of these data, such as uncertainty of measuring precise fascicle strains due to changes in pennation angle and the influence of changing pennation angle on force output, will introduce an unavoidable degree of error to the results, we feel they will have limited impact on the general conclusions drawn from the model. Indeed, re-running the model with larger maximum eccentric force values and increased resting length values resulted in only small changes in maximum force and maximum/minimum mechanical power output values recorded (Table 3) and did not influence the overall trends seen.

The results of the model indicate that the activation pattern influences the range of duty cycle and activation phase values over which maximum power output and total force can be generated. As the pattern of activation based on the soleus data resulted in a greater area under the curve (Fig. 1C,D), this activation pattern produced the highest total force and mechanical power output and a larger area in which maximum values could be attained. This indicates that for longer activation durations the precision of the timing and proportion of the stretch–shorten cycle the muscle is active may not be critical for maximum force or power production. By contrast, the model also indicated that subtle changes in activation phase and duty cycle could profoundly affect power production/absorption, as demonstrated by the position of the plantaris data in the contour plot (Fig. 10). The mechanical properties of the fibre were predicted to have the greatest influence on mechanical power output, where interestingly the fast fibre model predicted greater power absorption during the highest strain cycle (Fig. 10). In addition, the highest strains produced the greatest positive and negative power output values but not the greatest total force values (Fig. 9). The predictions of the model did not complement conclusions that may be drawn from observations of myoelectric timing and fascicle strain trajectories in each of the muscles. This was most evident in the results of the medial gastrocnemius where greater fascicle length changes at faster rates would suggest greater power output but the model indicated that power absorption occurred. It should be noted that the model was based on typical parameter values, consistent with past studies. It is possible, however, that variations in the chosen value of L_o or maximum eccentric force would affect the mechanical predictions. We tested this possibility by re-running the model twice more; firstly with L_o set to 15% longer, and secondly with maximum eccentric force set to 180% of σ_o. It was found that these alterations resulted in very limited changes in the resulting values (Table 3) or the contour plots, and that the general conclusions presented here were unchanged. We are therefore confident that our results represent fundamental differences in the functions of the physiologically distinct fibre type populations represented here by the different ankle extensor muscles of the rat.

CONCLUSION

The results indicate that there are significant differences in the mechanical behaviour and relative activation of the three ankle extensor muscles studied. Patterns of length change were not significantly influenced by changes in locomotor velocity or incline, while myoelectric duty cycle and activation and deactivation phases did change. This indicated that, under the conditions tested here, the relative timing of muscle activation was more influential on changes in mechanical force and/or power output than changes in the muscles' strain characteristics. This suggests that the skeletal anatomy of the limb constrains the *in vivo* muscle fascicle behaviour of all three muscles. The neuromuscular system however has many more degrees of freedom, and can vary the timing and level of muscle activation and the combination of motor units recruited across the three muscles, and may therefore drive modulations in force and power output required to meet any given locomotor demands. In agreement with this, the model indicated that subtle changes in activation phase and duty cycle could significantly influence levels of mechanical power output. Further work should focus on the interaction between synergistic muscles, the interaction between elastic and contractile muscle elements and consider the interaction between physiologically distinct compartments within a muscle.

LIST OF ABBREVIATIONS

a	normalised activation
A	cross-sectional area
c, s	magnitude constants
F	force
h	harmonic number
i	intensity
j	angle within the gait cycle
L	length
L_o	resting length
m	curvature of stress–strain relation
o	phase constant
P	mechanical power
r	roundness
s	width
t	time
u	neural excitation
w	skewness
β	ratio of activation to deactivation rate
ε	muscle fascicle strain
$\dot{\varepsilon}$	muscle fascicle strain rate
$\dot{\varepsilon}_o$	maximum strain rate
σ	isometric stress
σ_o	maximal isometric stress
τ_{act}	activation rate constant

ACKNOWLEDGEMENTS

E.H.T. is currently funded by a Sir Henry Wellcome Post-doctoral fellowship. Many thanks go to Michael Boyd and John Thurlborne for their help with surgical

procedures and care of the animals, Karin Jespers and Pattama Ritruechai for their help during data collection.

REFERENCES

Armstrong, R. B. and Phelps, R. O. (1984). Muscle fiber type composition of the rat hindlimb. *Am. J. Anat.* **171**, 259-272.
Aubert, X. (1956). Le couplage energetique de la contraction musculaire. Brussels: Editions Arscia.
Biewener, A. (1998). Muscle function *in vivo*: A comparison of muscles used for elastic energy savings *versus* muscles used to generate mechanical power. *Am. J. Zool.* **38**, 703-717.
Biewener, A. and Baudinette, R. (1995). *In vivo* muscle force and elastic energy storage during steady-speed hopping of tammar wallabies (*Macropus eugenii*). *J. Exp. Biol.* **198**, 1829-1841.
Biewener, A. and Roberts, T. J. (2000). Muscle and tendon contributions to force, work and elastic energy savings: a comparative perspective. *Exerc. Sport Sci. Rev.* **28**, 99-107.
Biewener, A., Corning, W. and Tobalske, B. (1998). *In vivo* pectoralis muscle force–length behavior during level flight in pigeons (*Columba livia*). *J. Exp. Biol.* **201**, 3293-3307.
Biewener, A. A., McGowan, C., Card, G. M. and Baudinette, R. V. (2004). Dynamics of leg muscle function in tammar wallabies (*M. eugenii*) during level *versus* incline hopping. *J. Exp. Biol.* **207**, 211-223.
Caiozzo, V. J., Herrick, R. E. and Baldwin, K. M. (1992). Response of slow and fast muscle to hypothyroidism: maximal shortening velocity and myosin isoforms. *Am. J. Physiol.* **263**, C86-C94.
Carroll, A. M. (2004). Muscle activation and strain during suction feeding in the largemouth bass *Micropterus salmoides*. *J. Exp. Biol.* **207**, 983-991.
Close, R. (1964). Dynamic properties of fast and slow skeletal muscles of the rat during development. *J. Physiol.* **173**, 74-95.
Close, R. and Luff, A. R. (1974). Dynamic properties of inferior rectus muscle of the rat. *J. Physiol.* **236**, 259-270.
Daley, M. A. and Biewener, A. A. (2003). Muscle force-length dynamics during level *versus* incline locomotion: a comparison of *in vivo* performance of two guinea fowl ankle extensors. *J. Exp. Biol.* **206**, 2941-2958.
De Ruiter, C. J., de Haan, A. and Sargeant, A. J. (1995). Physiological characteristics of two extreme muscle compartments in the medial gastrocnemius muscle of the rat. *Acta Physiol. Scand.* **153**, 313-324.
Delp, M. D. and Duan, C. (1996). Composition and size of type I, IIA, IID/X, and IIB fibers and citrate synthase activity of rat muscle. *J. Appl. Physiol.* **80**, 261-270.
Donley, J. M., Shadwick, R. E., Sepulveda, C. A., Konstantinidis, P. and Gemballa, S. (2005). Patterns of red muscle strain/activation and body kinematics during steady swimming in a lamnid shark, the shortfin mako (*Isurus oxyrinchus*). *J. Exp. Biol.* **208**, 2377-2387.
Edman, K. A., Elzinga, G. and Noble, M. I. (1978). Enhancement of mechanical performance by stretch during tetanic contractions of vertebrate skeletal muscle fibres. *J. Physiol.* **281**, 139-155.
Epstein, M. and Herzog, W. (1995). *Theoretical Models of Skeletal Muscle: Biological and Mathematical Considerations*. Chichester: John Wiley & Sons.
Fenn, W. O. (1924). The relation between the work performed and the energy liberated in muscular contraction. *J. Physiol.* **58**, 373-395.
Fukunaga, T., Kubo, K., Kawakami, Y., Fukashiro, S., Kanehisa, H. and Maganaris, C. N. (2001). *In vivo* behaviour of human muscle tendon during walking. *Proc. Biol. Sci.* **268**, 229-233.
Gabaldon, A. M., Nelson, F. E. and Roberts, T. J. (2004). Mechanical function of two ankle extensors in wild turkeys: shifts from energy production to energy absorption during incline *versus* decline running. *J. Exp. Biol.* **207**, 2277-2288.
Gillis, G. B. and Biewener, A. A. (2001). Hindlimb muscle function in relation to speed and gait: *in vivo* patterns of strain and activation in a hip and knee extensor of the rat (*Rattus norvegicus*). *J. Exp. Biol.* **204**, 2717-2731.
Gillis, G. B. and Biewener, A. A. (2002). Effects of surface grade on proximal hindlimb muscle strain and activation during rat locomotion. *J. Appl. Physiol.* **93**, 1731-1743.
Griffiths, R. I. (1991). Shortening of muscle fibres during stretch of the active cat medial gastrocnemius muscle: the role of tendon compliance. *J. Physiol.* **436**, 219-236.
Herzog, W. and Leonard, T. R. (2000). The history dependence of force production in mammalian skeletal muscle following stretch-shortening and shortening-stretch cycles. *J. Biomech.* **33**, 531-542.
Higham, T. E., Biewener, A. A. and Wakeling, J. M. (2008). Functional diversification within and between muscle synergists during locomotion. *Biol. Lett.* **4**, 41-44.
Hill, A. V. (1938). The heat of shortening and the dynamic constants of muscle. *Proc. Roy. Soc. Lond. B. Biol. Sci.* **126**, 136-195.
Hodson-Tole, E. F. and Wakeling, J. M. (2007). Variations in motor unit recruitment patterns occur within and between muscles in the running rat (*Rattus norvegicus*). *J. Exp. Biol.* **210**, 2333-2345.
Hodson-Tole, E. F. and Wakeling, J. M. (2008a). Motor unit recruitment patterns 1, Responses to changes in locomotor velocity and incline. *J. Exp. Biol.* **211**, 1882-1892.
Hodson-Tole, E. F. and Wakeling, J. M. (2008b). Motor unit recruitment patterns 2, The influence of myoelectric intensity and muscle fascicle strain rate. *J. Exp. Biol.* **211**, 1893-1902.
Hoffer, J. A., Caputi, A. A., Pose, I. E. and Griffiths, R. I. (1989). Roles of muscle activity and load on the relationship between muscle spindle length and whole muscle length in the freely walking cat. *Prog. Brain Res.* **80**, 75-85; discussion 57-60.
Lee, H. D. and Herzog, W. (2002). Force enhancement following muscle stretch of electrically stimulated and voluntarily activated human adductor pollicis. *J. Physiol.* **545**, 321-330.
Lichtwark, G. A. and Wilson, A. M. (2006). Interactions between the human gastrocnemius muscle and the Achilles tendon during incline, level and decline locomotion. *J. Exp. Biol.* **209**, 4379-4388.
Norenberg, K. M. and Fitts, R. H. (2004). Contractile responses of the rat gastrocnemius and soleus muscles to isotonic resistance exercise. *J. Appl. Physiol.* **97**, 2322-2332.
Otten, E. (1985). The jaw mechanism during growth of a generalised Haplochromis species: *H. elegans* Trewavas 1933 (Pisces, Cichlidae). *Netherlands J. Zool.* **33**, 44-98.
Otten, E. (1987). A myocybernetic model of the jaw system of the rat. *J. Neurosci. Methods* **21**, 287-302.
Roberts, T. J., Marsh, R. L., Weyand, P. G. and Taylor, C. R. (1997). Muscular force in running turkeys: the economy of minimizing work. *Science* **275**, 1113-1115.
Sanford, C. P. and Wainwright, P. C. (2002). Use of sonomicrometry demonstrates the link between prey capture kinematics and suction pressure in largemouth bass. *J. Exp. Biol.* **205**, 3445-3457.
Schiaffino, S. and Reggiani, C. (1996). Molecular diversity of myofibrillar proteins: gene regulation and functional significance. *Physiol. Rev.* **76**, 371-423.
Swoap, S. J., Caiozzo, V. J. and Baldwin, K. M. (1997). Optimal shortening velocities for *in situ* power production of rat soleus and plantaris muscles. *Am. J. Physiol.* **273**, C1057-C1063.
van Leeuwen, J. L. (1992). Muscle function in locomotion. In *Mechanics of Animal Locomotion*, vol. 11 (ed. R. McNeill Alexander). Berlin: Springer-Verlag.
von Tscharner, V. (2000). Intensity analysis in time-frequency space of surface myoelectric signals by wavelets of specified resolution. *J. Electromyogr. Kinesiol.* **10**, 433-445.
Wakeling, J. M. and Johnston, I. A. (1999). White muscle strain in the common carp and red to white muscle gearing ratios in fish. *J. Exp. Biol.* **202**, 521-528.
Woittiez, R. D., Baan, G. C., Huijing, P. A. and Rozendal, R. H. (1985). Functional characterisitcs of the calf muscles of the rat. *J. Morphol.* **184**, 375-387.
Zajac, F. E. (1989). Muscle and tendon: properties, models, scaling, and application to biomechanics and motor control. *Crit. Rev. Biomed. Eng.* **17**, 359-411.